Isovector parity mixing in ^{16}O investigated via the ^{15}N$(\vec{p},\alpha_0)^{12}$C resonance reaction

N. Kniest, M. Horoi,* O. Dumitrescu,* and G. Clausnitzer

Institut für Kernphysik, Strahlenzentrum der Universität Giessen, D-6300 Giessen, Germany

(Received 10 September 1990)

The parity- and isospin-forbidden α_0 decay from ^{16}O*$(J^{\pi}=2^-$, $T=1$, $E_x=12.9686$ MeV) to ^{12}C(g.s.) has been investigated theoretically. Considering various strong and weak interaction models the longitudinal A_L and the irregular transverse A_b analyzing powers of the reaction ^{15}N$(\vec{p},\alpha_0)^{12}$C have been calculated in the energy range of the 2^- resonance in ^{16}O*. Energy anomalies for the expected interference effects, relevant for experiments, have been found to be $A_L=1.1\times10^{-5}$ and $A_b=0.9\times10^{-5}$ at $\theta=90°$ and $A_L=1.4\times10^{-5}$ and $A_b=0.2\times10^{-5}$ at $\theta=150°$ based on a conservative value of 0.1 eV for the parity-nonconservation matrix element. A proposal for an experimental investigation is sketched.

I. INTRODUCTION

Parity nonconservation (PNC) in nuclear reactions involving hadrons or nuclei is commonly attributed to the weak-hadron interaction. The weak interaction between the nucleons, and especially those components with dominant contribution due to neutral weak currents, can only be studied in flavor-conserving processes, restricting all investigations to low-energy nuclear physics (for a recent review article, see, e.g., Ref. [1]). The weak nucleon-nucleon (NN) interaction is only of the order of 10^{-7} compared to strong interactions. Therefore, only small effects are expected and measured in few nucleon systems (see, e.g., Ref. [2]). However, for nuclei in the mass region $A=14$–21, substantial enhancements of PNC effects are predicted [1,3] and observed (see, e.g., Ref. [1]). The enhancement of these effects originates from several reasons, the most important being the small level spacing (e.g., only 20 keV [4,5]) between nuclear states of the same spin and opposite parity in the compound nucleus involved. The next important reason arises from the possible increase of the ratio between parity-forbidden and parity-allowed transition-matrix elements caused by the nuclear structure of the states involved [1,3,6,7]. The same conditions which generate the enhancement, sometimes, complicate a reliable determination of the nuclear matrix elements theoretically. Therefore, it is necessary to select exceptional cases, in which the nuclear structure calculations can be done reliably. This is the case for closely spaced doublets of the same spin and opposite parity located far away from other similar levels. In this case the parity impurities are well approximated by two-state mixing, which simplifies the analysis. If these two states can be populated selectively in a nuclear reaction, one can even perform measurements which are sensitive to only one special isospin component of the PNC-NN interaction. Moreover, the use of polarized particles has the advantage that an interference effect between PNC and parity-conservation (PC) amplitudes can be observed.

In the present paper the α_0 transition from the $J^{\pi}T=2^-1$ state in ^{16}O ($E_x=12.9686$ MeV, $\Gamma_{c.m.}=1.6\pm0.1$ keV), populated by resonant capture of polarized protons ($E_p=0.898$ MeV), to ^{12}C(g.s.) is investigated theoretically. This transition was originally mentioned by Bizzeti and Maurenzig [7]. The α_0 transition is forbidden by parity and isospin selection rules. It therefore can predominantly be described by the isovector part of the PNC-NN potential, i.e., one-pion exchange, thus being sensitive to the weak πNN coupling constant h_π, the size of which may be related to the presence of neutral currents in the hadronic weak interaction.

The excitation function of the PNC longitudinal (A_L) and PNC transverse (A_b) analyzing powers [7,8] are expected to show an energy anomaly at the 2^-1 resonance energy as a result of the interference of the forbidden (PNC: 2^-1, 12.9686 MeV) and allowed (PC: 2^+0, 13.020 MeV; 1^-1, 13.090 MeV) resonance transition amplitudes as well as a (PC: 0^+0) background transition amplitude. The level structure of the ^{16}O nucleus enhances the interference effect because of the close-lying ($\Delta E=51$ keV) broad overlapping 2^+0 state at $E_x=13.020$ MeV with $\Gamma_{c.m.}=150\pm10$ keV [9]. Furthermore, the PNC α_0 transition can be studied selectively via the ^{15}N$(\vec{p},\alpha_0)^{12}$C resonance reaction with two independent observables, namely, the PNC longitudinal (A_L) and PNC transverse (A_b) analyzing powers.

The aim of this paper, therefore, is to give the basic formulas for these and other related observables (Secs. II and III) and the large-scale shell-model predictions for the PNC matrix elements (Sec. IV), used to calculate the energy anomalies in the excitation functions of the analyzing powers (Sec. V). These results have been taken into account for discussing the basic ideas toward an experimental investigation. A conclusion with outlook is given in Sec. VI.

II. NUCLEAR REACTION CROSS SECTION AND ANALYZING POWERS

Consider a proton beam with the polarization vector $\mathbf{P}=\langle 2\mathbf{S}_p\rangle$, which travels along the z axis to the unpolar-

ized target nucleus of spin $I = \frac{1}{2}$. In this case the resonance reaction cross section is

$$\frac{d\sigma}{d\Omega} = \sigma_{un}(1 + \mathbf{A} \cdot \mathbf{P}) , \tag{1}$$

where

$$\sigma_{un} = \mathrm{Tr}(TT^+) = \sigma_0^{(0)} \tag{2}$$

is the differential cross section for the resonance reaction induced by an unpolarized proton beam. The vector analyzing powers are given by [6]

$$\mathbf{A} = \sigma_{un}^{-1}\mathrm{Tr}(T2\mathbf{S}_p T^+) = 2\sum_{\kappa} \sigma_{\kappa}^{(1)}\mathbf{e}^{\kappa}(\sigma_0^{(0)})^{-1} , \tag{3}$$

with

$$A_L = 2\,\mathrm{Re}\sigma_0^{(1)}(\sigma_0^{(0)})^{-1} , \tag{4}$$

$$A_b = -2\sqrt{2}\,\mathrm{Re}\sigma_1^{(1)}(\sigma_0^{(0)})^{-1} , \tag{5}$$

$$A_n = -2\sqrt{2}\,\mathrm{Im}\sigma_1^{(1)}(\sigma_0^{(0)})^{-1} . \tag{6}$$

where A_L is the PNC longitudinal, A_b is the PNC transverse, and A_n is the PC transverse analyzing power,

$$\mathbf{e}^1 = -2^{-1/2}(\mathbf{e}_b - i\mathbf{e}_n), \quad \mathbf{e}^0 = \mathbf{e}_L, \quad \mathbf{e}^{-1} = 2^{-1/2}(\mathbf{e}_b + i\mathbf{e}_n) \tag{7}$$

are the cyclic contravarient unit vectors [10], and

$$\mathbf{e}_L = \mathbf{k}_i(k_i)^{-1}, \quad \mathbf{e}_n = \mathbf{k}_i \times \mathbf{k}_f(|\mathbf{k}_i \times \mathbf{k}_f|)^{-1}, \quad \mathbf{e}_b = \mathbf{e}_n \times \mathbf{e}_L \tag{8}$$

are the unit vectors of the reference frame given by the Madison convention [11]. The common quantity in Eqs. (3)–(6) is defined [6] as

$$\sigma_{\kappa}^{(v)} = k_i^{-2} \sum_{Jlsl_1s_1J'l'l_2s_2L} E_{Jlsl_1s_1,J'l'sl_2s_2}^{(v,\kappa)}(L)P_L^{\kappa}(\cos(\theta_f))T_{\beta ls,\beta_1,l_1s_1}^{J\pi}(T_{\beta'l's,\beta_2l_2s_2}^{J\pi})^* , \tag{9}$$

where $P_L^{\kappa}(\cos(\theta))$ are the associated Legendre polynomials, and $T_{\beta ls,\beta_1 l_1 s_1}$ are the T matrices, discussed in Sec. III. The quantities

$$E_{Jlsl_1s_1,J'l'sl_2s_2}^{(v,\kappa)}(L) = 16^{-1}\langle\tfrac{1}{2}||O^v||\tfrac{1}{2}\rangle(-1)^{\kappa-J-s-l_2-s_2+L}\hat{l}_1\hat{l}_2\hat{s}_1\hat{s}_2\hat{l}\hat{l}'\,\hat{L}^2\hat{J}^2\hat{J}'^2$$

$$\times\sqrt{(L-\kappa)!/(L+\kappa)!}\,W(JlJ'l';sL)W(\tfrac{1}{2}\tfrac{1}{2}s_1s_2;v\tfrac{1}{2})\begin{bmatrix} ll'L \\ 000 \end{bmatrix}\sum_j(-1)^j\hat{j}^2\begin{bmatrix} L & v & j \\ \kappa & -\kappa & 0 \end{bmatrix}\begin{bmatrix} l_1l_2j \\ 0\,0\,0 \end{bmatrix}\begin{bmatrix} l_1l_2j \\ s_1s_2v \\ JJ'L \end{bmatrix} \tag{10}$$

are the corresponding geometrical coefficients [6] with

$$O^{(v)} = \begin{cases} 1, & v=0 \\ \mathbf{S}, & v=1 \end{cases}, \tag{11}$$

and

$$\langle\tfrac{1}{2}||1||\tfrac{1}{2}\rangle = 1, \quad \langle\tfrac{1}{2}||S^{(1)}||\tfrac{1}{2}\rangle = \frac{\sqrt{3}}{2} . \tag{12}$$

The quantities β in Eq. (9) denote all remaining quantum numbers that specify the channel states (e.g., names, spin, and parities of the fragments). In the applications we shall denote the proton channel with p and the α channel with α.

III. T MATRICES FOR THE $^{15}\mathrm{N}(\vec{p},\alpha_0)^{12}\mathrm{C}$ RESONANCE REACTION

The expressions derived in the preceding section are applied for the $^{15}\mathrm{N}(\vec{p},\alpha_0)^{12}\mathrm{C}$ reaction via the 2^-1, $E_x = 12.9686$ MeV level in $^{16}\mathrm{O}$. It is found that the PNC transition amplitude of the 2^-1 level shows a significant interference only with those allowed transition amplitudes involving the 2^+0, $E_x = 13.020$ MeV and 1^-1, $E_x = 13.090$ MeV resonance levels, and a background 0^+0 transition amplitude. Because of the small proton energy, the angular momentum can be restricted to $l \leq 2$. Together with the spins and parities of the involved nuclei, the following four PC transition amplitudes are allowed, denoted by a small t:

$$t_1 = T_{bg} = T_{\alpha00,p11}^{0^+}, \quad t_2 = T_{\alpha10,p01}^{1^-}, \quad t_3 = T_{\alpha10,p21}^{1^-}, \quad t_4 = T_{\alpha20,p11}^{2^+} . \tag{13}$$

Two PNC transition amplitudes, denoted by a capital T, are taken into account:

$$T_1 = T^{2^+,-}_{\alpha20,p20}, \quad T_2 = T^{2^+,-}_{\alpha20,p21} \ . \tag{14}$$

The PC resonance T-matrix elments can be expressed in the form [6]

$$T^{J\pi}_{\alpha ls, pl_1 s_1} = i \exp(i\xi_{\alpha ls})(\Gamma^{J\pi}_{\alpha ls})^{1/2}(\Gamma^{J\pi}_{pl_1 s_1})^{1/2}\exp(i\xi_{pl_1 s_1}) \left[E - E^{J\pi} + \frac{i}{2}\Gamma^{J\pi}\right]^{-1} , \tag{15}$$

while for a two-level system of the same spin and opposite parity, the PNC T-matrix elements have the following expression:

$$T^{J\pi,-\pi}_{\alpha ls, pl_1 s_1} = i \exp(i\xi_{\alpha ls})(\Gamma^{J-\pi}_{\alpha ls})^{1/2}\langle J^{-\pi}|H_{\mathrm{PNC}}|J^\pi\rangle(\Gamma^{J\pi}_{pl_1 s_1})^{1/2}\exp(i\xi_{pl_1 s_1}) \left[E - E^{J-\pi} + \frac{i}{2}\Gamma^{J-\pi}\right]^{-1}\left[E - E^{J\pi} + \frac{i}{2}\Gamma^{J\pi}\right]^{-1} . \tag{16}$$

$\xi_{\alpha(p)ls}$, $E^{J\pi}$, and $\Gamma^{J\pi}$ stand for the $\alpha(p)$-channel phases, resonance energies, and total resonance widths, respectively. E is the proton energy in the compound system. The quantities $(\Gamma^{J\pi}_{\alpha(p)ls})^{1/2}$ are taken from experiments (see Ref. [9]) if available; otherwise, they are expressed in terms of the OXBASH spectroscopic amplitudes [12], geometrical coefficients, and experimental total channel widths.

The calculations within the OXBASH code gave the following results:

$$\left|\frac{(\Gamma^{1^-}_{P_{21}})^{1/2}}{(\Gamma^{1^-}_{P_{01}})^{1/2}}\right| = 2\times10^{-3}, \quad \Gamma^{1^-}_{P_{01}} \simeq \Gamma^{1^-}_p(\mathrm{exp}) = 100 \ \mathrm{keV} , \tag{17}$$

$$\left|\frac{(\Gamma^{2^-}_{P_{20}})^{1/2}}{(\Gamma^{2^-}_{P_{21}})^{1/2}}\right| = 1, \quad \Gamma^{2^-}_{P_{20}} = \Gamma^{2^-}_{P_{21}} = \tfrac{1}{2}\Gamma^{2^-}_p(\mathrm{exp}) = 0.495 \ \mathrm{keV} . \tag{18}$$

It turns out that $T_1 = T_2$. Contributions from the spin-orbit potential to the proton channel phases and spectroscopic amplitudes have been neglected because of the low proton energy ($E_p \simeq 900$ keV). In the vicinity of the 2^-1 narrow resonance, the analyzing powers A_L and A_b have the following simple expression:

$$A_{L(b)} = D_{L(b)}\mathrm{Re}\left[\frac{1}{2}\Gamma^{2^-}\left[E - E^{2^-} + \frac{i}{2}\Gamma^{2^-}\right]^{-1}\exp[i(\phi_{L(b)} + \phi_{\mathrm{PNC}})]\right] , \tag{19}$$

where ϕ_{PNC} is the phase of the PNC matrix element. The quantity $D_{L(b)}$ is given by

$$D_{L(b)} = 2(\Gamma^{2^-})^{-1}|\langle2^-1|H_{\mathrm{PNC}}|2^+0\rangle|\sqrt{\Gamma^{2^-}_p/2\Gamma^{2^+}_p}|C_{L(b)}| , \tag{20}$$

where

$$C_{L(b)} = |C_{L(b)}|\exp(i\phi_{L(b)}) = 2\left[\sum_l P^{(\kappa)}_l(\cos\theta)\sum_n b^l_n(L(b))\tilde{t}_4 t^*_n\right]\left[\sum_l P_l(\cos\theta)\sum_{mn} a^l_{mn}t_m t^*_n\right]^{-1} \tag{21}$$

is a function on the PC transition-matrix elements [see Eq. (13)] only (for L, $\kappa = 0$; for b, $\kappa = 1$, $\tilde{t}_4 = t_4\exp[i(\xi_{P_{21}} - \xi_{P_{11}})]$). The coefficients $b^{(l)}_n(L(b))$ and $a^{(l)}_{mn}(L(b))$ are simple specific values of the $E^{(v,\kappa)}$ geometrical coefficients [see Eq. (10)]. In the α-channel case, the spectroscopic amplitudes are incorporated in the experimental partial α widths. The background transition-matrix element [see Eq. (13)] is a simple complex number.

From Eq. (24) of Ref. [13], it is possible to extract the weight of the admixtures from different 2^+0 levels to the 2^-1 level as a product:

$$F_n S^{1/2}_{\alpha n} = |(E^{2^-1} - E^{2^+0})^{-1}\langle2^11|H_{\mathrm{PNC}}|2^+_n0\rangle S^{1/2}_{\alpha n}| , \tag{22}$$

where $S^{1/2}_{\alpha n}$ is a SU(3) alpha-particle amplitude [12]. The results are listed in Table I. From these values we conclude that the assumption of a parity-mixed doublet (2^-1, 12.9686 MeV and 2^+0, 13.020 MeV excited states

TABLE I. Quantity $S^{1/2}_{\alpha n}F_n$ as defined in Eq. (22), which measures the contributions of different 2^+0 levels in the parity mixing of the 2^-1, $E_x = 12.9686$ MeV level in ^{16}O*.

E^{exp}_x (MeV)	$10^6 F_\alpha S^{1/2}_\alpha$
6.9171	0.009 2704
9.8445	0.011 6097
11.5200	0.018 4660
13.0200	0.766 3424
14.9260	0.006 7910
15.2600	0.006 7910

TABLE II. Resonance parameters of the ^{16}O excited states involved in the calculations of the cross section and analyzing powers of the $^{15}N(\vec{p},\alpha_0)^{12}C$ resonance reaction [9].

$J^{\pi}T$	E_x^{exp} (MeV)	E_p^{lab} (MeV)	E_α^{lab} (MeV)	$\Gamma_{c.m.}$ (keV)	Γ_α (keV)	Γ_p (keV)
2^-1	12.9686	0.8971	7.7422	1.6		0.99
2^+0	13.0200	0.9519	7.8107	150.0	146.6	3.40
1^-1	13.0900	1.0266	7.8770	130.0	30.0	100.00

in ^{16}O) is justified. In this case the expression of Eq. (16) for the T matrices, obtained by expanding the exact Green's function [6,14] to first order in H_{PNC}, is certainly a good approximation. It is assumed that the projectile and target are parity eigenstates. Then PNC contributions from direct reaction terms are ignored and only effects related to the closeness of the two resonances are taken into account. The resonance parameters for the quantities entering in Eqs. (13) and (14) are give in Table II and Fig. 1. The parity mixing of the above-mentioned doublet is of particular interest because of the following reasons.

(1) The mixing is sensitive to the $\Delta T = 1$ components of H_{PNC} and especially to the part described by weak pion exchange, taking the quark model picture. In this case quantitative information about neutral current contributions to H_{PNC} is expected. Several cases have been proposed theoretically, but only few of them have been experimentally investigated; only the ^{18}F experiments (average of five investigations [1]) give a reliable upper limit for the weak-pion nucleon coupling constant, especially due to the relatively model-independent way to extract the PNC matrix element from the first forbidden β decay rate of ^{18}Ne (see Ref. [1] and references therein). However, the result for the coupling constant is in contradiction to the predictions of Ref. [15] and a recent calculation of Ref. [16]. Therefore, additional investigations are necessary, especially with independent observables. PNC experiments via $(\vec{p},\alpha)$ reactions have the advantages that nuclear levels can be populated selectively and different observables can be measured using polarized projectiles. Up to now, only the case of the $^{19}F(\vec{p},\alpha_0)^{16}O$ reaction has been studied experimentally [4,5,17], giving an upper limit [4].

(2) The polarization observables for the $^{15}N(\vec{p},\alpha_0)^{12}C$ reaction provide a favorable way to determine the PNC matrix elements. The energy anomaly in the PNC analyzing powers (A_L and A_b) is magnified by nuclear structure effects in addition to the 51-keV energy difference between the levels involved. The magnification arises from coherent contributions of proton and α channels. The quantity $C_{L(b)}$ describes the ratio between the PC–T-matrix contribution to the PNC analyzing powers and the (unpolarized) cross section for the $(\vec{p},\alpha)$ reaction [see Eq. (21)]. The value of this ratio is about 0.1 in the resonance region, being a measure for the coherent effect. The width of the 2^-1 resonance level is very small (1.6 keV) and acts as an enhancement factor, too [see Eq. (20) and Sec. V]. The ratio $\Gamma_p^{2^-}/\Gamma_p^{2^+}$ has a value close to unity (see Table II) and is another enhancement factor, as pointed out in Ref. [3] (similar ratios of unnatural to nat-

ural parity-level widths are of the order of 10^{-1}; see, e.g., Refs. [6,9]). The PC matrix elements t_2 and t_3 have nearly the same magnitude, while t_4 is two orders of magnitude less than t_2.
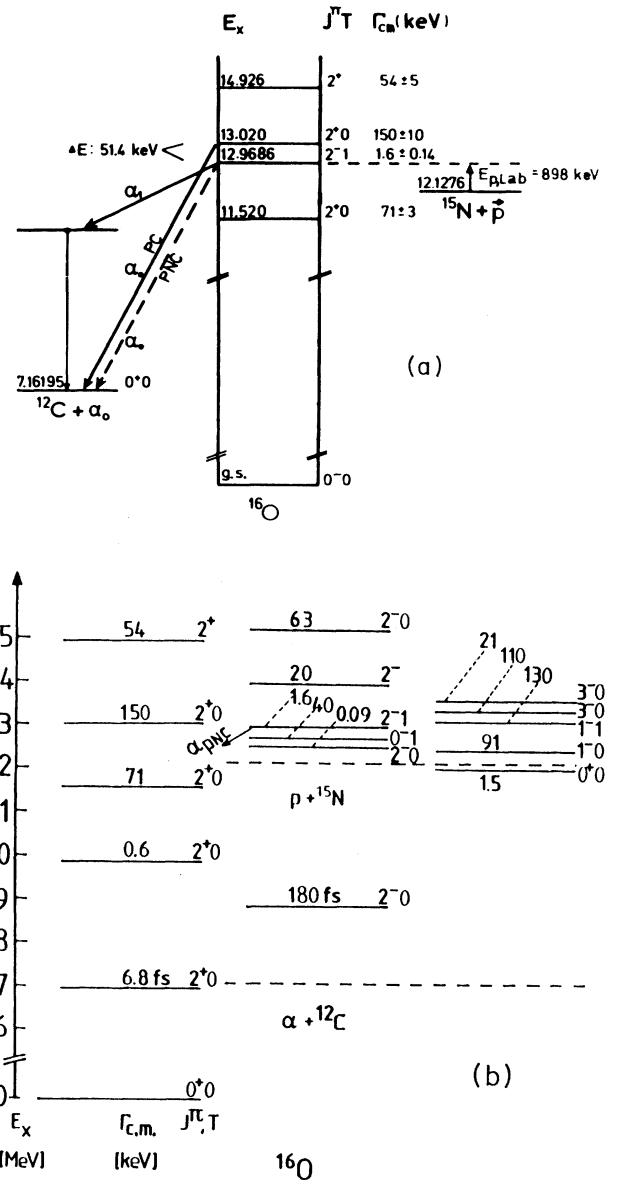
FIG. 1. Relevant ^{16}O levels for calculating the PNC analyzing powers of the $^{15}N(\vec{p},\alpha_0)^{12}C$ reaction in the vicinity of the 2^-1 resonance.

E_x[MeV]
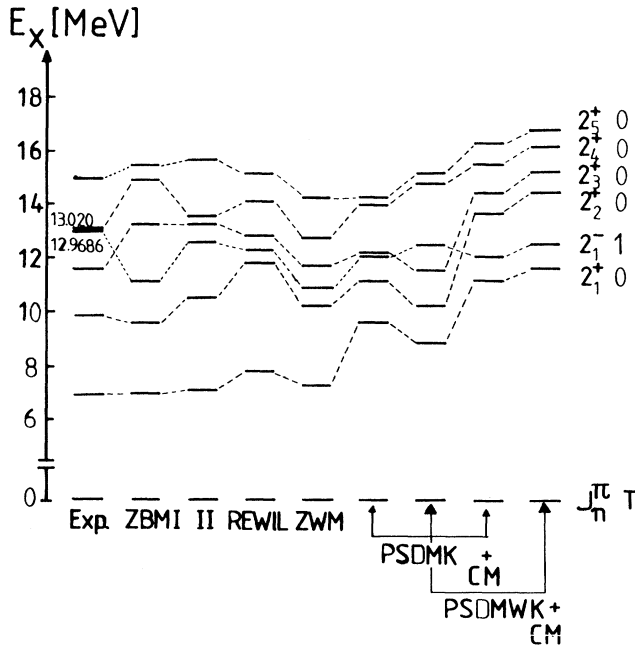
FIG. 2. First five 2^+0 and first 2^-1 excited levels in ^{16}O*, taken from experiment and calculated within different models of the OXBASH code.

(3) The cross section for the ^{15}N($\vec{p},\alpha_0$)^{12}C case is maximal at backward angles [18]. Moreover, the normal PC analyzing power is negligible small [18] in this energy region for large scattering angles, which is a favorable situation for measurement. Furthermore, the α channel can be studied more precisely than is, e.g., the case with PNC elastic scattering (target impurities, reduced number of α channels).

(4) The PNC α_0 transition can be studied via the ^{15}N($\vec{p},\alpha_0$)^{12}C resonance reaction with two polarization observables, namely, the PNC longitudinal and PNC transverse analyzing powers A_L and A_b. Information about the PNC matrix element can be obtained independently from the excitation energy of each observable.

(5) The theoretical models, included in the OXBASH code, are reasonably good (see Fig. 2) for the levels of the mentioned $2^-,2^+$ doublet, since the even-even ^{16}O nucleus is an often-used candidate being well described by such realistic models. Especially, the (first) excited $J^\pi=2^-1$ state can reliably be reproduced.

In the following section we discuss the degree of accuracy of the shell-model calculations within the available OXBASH code in order to substantiate the opinion that the experimental results on PNC analyzing powers of the ^{15}N($\vec{p},\alpha_0$)^{12}C resonance reaction with $E_p \simeq 0.898$ MeV can be analyzed free from nuclear uncertainties.

IV. SHELL-MODEL PREDICTION FOR THE ISOVECTOR PNC MATRIX ELEMENT

In order to predict the magnitude of the effect and to check the feasibility of an experiment to measure A_L

and/or A_b around the resonance energy of the first excited 2^-1 state in ^{16}O, we calculated the

$$\langle 2^-1,\ 12.9686\ \text{MeV}|H_{\text{PNC}}|2^+0,\ 13.020\ \text{MeV}\rangle$$

matrix element using the OXBASH code in the Michigan State University version [12], which includes different model spaces and different residual effective two-nucleon interactions.

Two different model spaces have been used: the ZBM model space, which contains the $p_{1/2}$, $1d_{5/2}$, and $2s_{1/2}$ orbits in the valence space, and the PSD model space, including, in addition, the $1p_{3/2}$ and $1d_{3/2}$ orbits. In order to maintain the matrix dimensions at a nonprohibited level, the nucleons have been considered to be frozen in the $1p_{3/2}$ orbit; thus a fixed $(1s_{1/2})^4(1p_{3/2})^8$ configuration is assumed in all cases. It turns out that at least four-particle–four-hole calculations are needed [1,19] in order to describe the 2^+ states in ^{16}O.

Four different residual interactions have been used in ZBM model space: ZBM I and ZBM II are the interactions I and II from Zuker, Buck, and McGrory [20,21]; REWIL and ZWM are the F and Z interactions, respectively, from McGrory and Wildenthal [22]. Two different combinations of interactions have been taken into account in the PSD model space: PSDMK is a Cohen-Kurath [23] interaction for $1p$ orbits plus a Preedom-Wildenthal [24] interaction for sd orbits and Millener-Kurath [25] matrix elements between p and sd orbits. PSDMWK is similar to PSDMK, except the Wildenthal W interaction [26,27] is taken for the sd subspace. While the center-of-mass spuriosity is small in the ZBM model space [28], the number of spurious components is high in the PSD space, but the degree of spuriosity of every component is small. In PSDMK+CM and PSDMWK+CM, the contributions of spurious components were eliminated with a procedure analyzed in Ref. [29].

There are two types of contributions to the PNC matrix element: One is coming from two-body transition densities (TBTD's), if all four orbitals entering the two-body matrix elements (TBME's) are in the valence space [30]; another one arises from the one-body transition densities (OBTD's) if two orbitals are in the core. The only contribution to the latter one comes from the matrix element

$$\langle(1s_{1/2})^4(1p_{3/2})^82s_{1/2}\|H_{\text{PNC}}\|(1s_{1/2})^4(1p_{3/2})^81p_{1/2}\rangle ,$$

(23)

which turns out to be the dominant one in all described cases.

The TBME's have been calculated with harmonic-oscillator wave functions ($\hbar\omega=14$ MeV is appropriate for $A=16$) [30]. The magnitude of the matrix element depends on the type of the radial wave functions due to the effect of the derivative operator. The values calculated with more realistic Woods-Saxon single-particle wave functions have been found to be at most 20% smaller than those from the harmonic-oscillator approximation. Because of the short-range contribution of heavy-meson

exchange to H_{PNC}, short-range correlations (SRC) of the shell-model wave function must be implemented. This has been done multiplying the radial two-body wave function by a kind of Jastrow factor [31]:

$$1 - \exp(-ar^2)(1 - br^2),$$

$$a = 1.1 \text{ fm}^{-2},$$

(24)

$$b = 0.68 \text{ fm}^{-2}.$$

This procedure results in a suppression of the pion-exchange matrix element by 20%–30% and a decrease for ρ- and ω-exchange matrix elements by a factor of 3–4. Similar results have been obtained with a much more elaborate treatment of SRC such as the Bethe-Goldstone approach [32–34].

While the form of the one-boson exchange PNC-NN potential is well established (see, e.g., Refs. [33,35]), the weak meson-nucleon-nucleon (MNN) coupling constants have been the subject of debate in the recent years in particle physics [15,16,33,35,36] as well as in low-energy nuclear physics [1]. Investigating the PNC-MNN vertices within the framework of a nonlinear chiral effective Lagrangian, Kaiser and Meissner [16] (KM) reported a considerably smaller value (2.0×10^{-8}) for the weak πNN coupling constant (h_π) compared to the recent result

TABLE III. Weak meson-nucleon coupling constants calculated within different weak-interaction models (in units of 10^{-7}). The abbreviations are given in the text.

$h_{\text{meson}}^{\Delta T}$	KM	DDH	AH	DZ
h_π^1	0.19	4.54	2.09	1.3
h_ρ^0	−3.70	−11.40	−5.77	−8.3
h_ρ^1	−0.10	−0.19	−0.22	0.39
h_ρ^2	−3.30	−9.50	−7.06	−6.7
$h_{\rho'}^1$	−2.20	0	0	0
h_ω^0	−1.40	−1.90	−4.97	−3.9
h_ω^1	−1.00	−1.10	−2.39	−2.2

(1.3×10^{-7}) obtained by Dubovik and Zenkin [36] (DZ) in Weinberg-Salam theory plus quark model, both significantly lower than the often used Desplanques-Donoghue-Holstein (DDH) best value [15] (4.6×10^{-7}). Moreover, the weak couplings extracted from low-energy experiments by Adelberger and Haxton [1] (AH) are close to the DZ [36] values (see Table III). This controversy was a stimulation for an analysis of the PNC matrix elements based on all four models, in order to search for
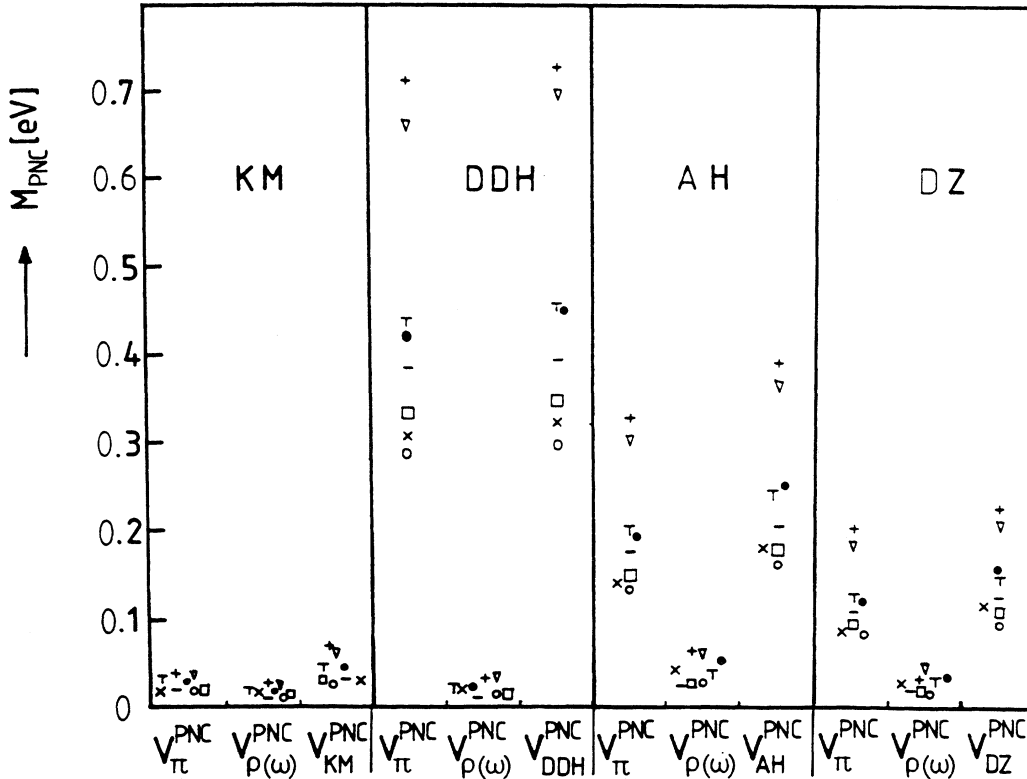
FIG. 3. PNC matrix element calculated within different strong- and weak-interaction models. The abbreviations are given in the text. The symbols refer to the following models: ○: ZBM I; ▽: ZBM II; □: REWIL; +: ZQM; −: PSDMK; ×: PSDMK + CM; T: PSDMWK; ●: PSDMWK + CM.

TABLE IV. Values of the PNC-NN matrix element (in eV) between the 2^-1, 12.9686 MeV state and the 2^+0, 13.020 MeV state in ^{16}O calculated within different models for weak and strong interactions. The abbreviations are given in the text.

Interactions	KM V_π	KM $V_{\rho(\omega)}$	V_{tot}^{KM}	DDH V_π	DDH $V_{\rho(\omega)}$	V_{tot}^{DDH}	AH V_π	AH $V_{\rho(\omega)}$	V_{tot}^{AH}	DZ V_π	DZ $V_{\rho(\omega)}$	V_{tot}^{DZ}
ZBM I	−0.0167	−0.0116	−0.0283	−0.287	−0.016	−0.303	−0.138	−0.028	−0.166	−0.086	−0.021	−0.107
ZBM II	0.0370	0.0257	0.0627	0.660	0.036	0.696	0.306	0.061	0.367	0.189	0.047	0.236
REWIL	0.0186	0.0123	0.0309	0.332	0.017	0.349	0.154	0.290	0.183	0.095	0.023	0.118
ZWM	−0.0397	−0.0268	−0.0665	−0.709	−0.037	−0.746	−0.328	−0.064	−0.392	−0.204	−0.050	−0.254
PSDMK	−0.0212	−0.0115	−0.0321	−0.381	−0.014	−0.395	−0.176	−0.029	−0.205	−0.109	−0.022	−0.131
PSDMK+CM	0.0169	0.0162	0.0331	0.304	0.021	0.325	0.141	0.041	0.182	0.087	0.031	0.118
PSDMWK	0.243	0.0162	0.0405	0.437	0.020	0.457	0.202	0.040	0.242	0.125	0.031	0.156
PSDMWK+CM	0.0235	0.0195	0.0430	0.423	0.025	0.448	0.196	0.049	0.245	0.122	0.037	0.159

new experimentally accessible cases, being sensitive to (h_π) and theoretically clean (i.e., uncertainties from nuclear structure calculations are small).

In the present calculation the standard form for H_{PNC} has been used [15] [see also Eqs. (27)–(36)] with the weak-coupling constants given in Table III. The strong-coupling constants are summarized in the last four columns of Table II from Ref. [16]. The calculated matrix elements for different weak-interaction models and different shell-model residual interactions are shown in Table IV and Fig. 3. The matrix elements are calculated up to an i phase. Their signs are due to the OXBASH wave-function phases and are kept for further references. Nevertheless, the difference between the maximum and the minimum of the analyzing power does not depend on the phase of the PNC matrix element (see Sec. V). As can be seen, the results for different interactions agree within a factor of 2.5 and no large suppression appears when the model space is enlarged. The ρ- and ω-exchange contributions add coherently to the total matrix element in every case. The contributions from heavy mesons do not exceed 25% for the DDH, AH, and DZ cases, but increase to 50% in the KM model, reducing the contribution of pion exchange. If this model is taken at face value, the chance to observe a trace of h_π is considerably decreased.

Considering the present discrepancies between the DDH values [15] and the KM [16] results, the conservative choice of the matrix element $\langle 2^-1|H_{PNC}|2^+0\rangle \simeq 0.1$ eV is consistent with the DZ [36] model and is also supported by $\Delta T = 1$ PNC experiments [1,37,38]. In this case 75% of the value arises from pion exchange. The contribution of the new class of diagrams in the PNC single-particle Hamiltonian, recently proposed by Caprini and Micu [39], vanishes for the proposed matrix element.

V. LONGITUDINAL AND IRREGULAR TRANSVERSE ANALYZING POWERS FOR THE ^{15}N($\vec{p}, \alpha_0$)^{12}C RESONANCE REACTION

It is essential to compare the predictions of the theoretical model introduced in Secs. II an III with the experimental results for the cross section and the (regular) analyzing power for the ^{15}N(p, α)^{12}C reaction. The reso-

nance parameters for the used PC T matrices [Eqs. (13) and (15)], taken from the latest compilation [9], are given in Table II. The proton phases ξ_{pls} have been calculated within a folding procedure, using a realistic M3Y interaction [40], derived from G-matrix elements based upon the Reid NN potential and the Sussex matrix elements [41]. The results are very close to the Coulomb phases (see Table V). The α-channel phases and the background PC 0^+0 T-matrix element $t_1 = t \exp[i(\alpha)]$ have been fitted (see Table V) to reproduce the Legendre polynomial coefficients for the cross section and PC analyzing power of Pepper and Brown [18]. The expansion coefficients extracted from experiment and from the present investigation are given in Table VI. Figure 4 shows the quality of the theoretical treatment. The calculation of the PNC analyzing powers A_L and A_b has been performed with the same parameters. Figure 5 shows (on an expanded horizontal scale) the predicted size of the quantities A_L and A_b around the narrow 2^-1 resonance ($E_p \approx 898$ keV), relevant for an experiment to determine the PNC
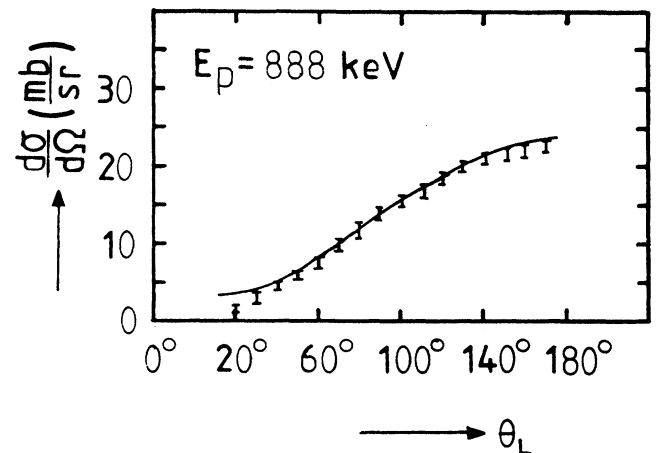
FIG. 4. Angular distribution of the differential cross section at $E_p = 888$ keV. The circles are taken from Ref. [18]; the solid line follows from the present prediction.

N. KNIEST, M. HOROI, O. DUMITRESCU, AND G. CLAUSNITZER

TABLE V. Proton- and α-channel phases as well as the PC 0^+0T-matrix element calculated with the M3Y interaction or fitted to the experimental data as explained in the text $t_1 = t\,\exp(i\alpha)(t=0.1,\ \alpha=0)$.

$\xi^{1-}_{\alpha_{10}}$	$\xi^{2+}_{\alpha_{20}}$	$\xi^{1-}_{p_{01}}$	$\xi^{1-}_{p_{21}}$	$\xi^{2+}_{p_{11}}$	$\xi^{2-}_{p_{20}}$	$\xi^{2-}_{p_{21}}$
5.6548	1.25664	−0.200	1.119	0.5855	1.119	1.119

matrix element. These predictions are based on the size of 0.1 eV for the PNC matrix element, which is a conservative estimate, as can be verified, e.g., from Fig. 3 and Table IV. Other results for all models, given in Table IV, can be obtained by straightforward multiplication.

The PNC analyzing power shows a dispersionlike energy behavior around the resonance energy, the form depending on the phase difference of the contributing matrix elements (see Fig. 5). However, the difference between the maximum and the minimum (denoted by $\Delta A_{L(b)}$ in Fig. 5) is equal to the quantity $D_{L(b)}$ defined in Eq. (20). It is a very important fact that $\Delta A_{L(b)}$ depends
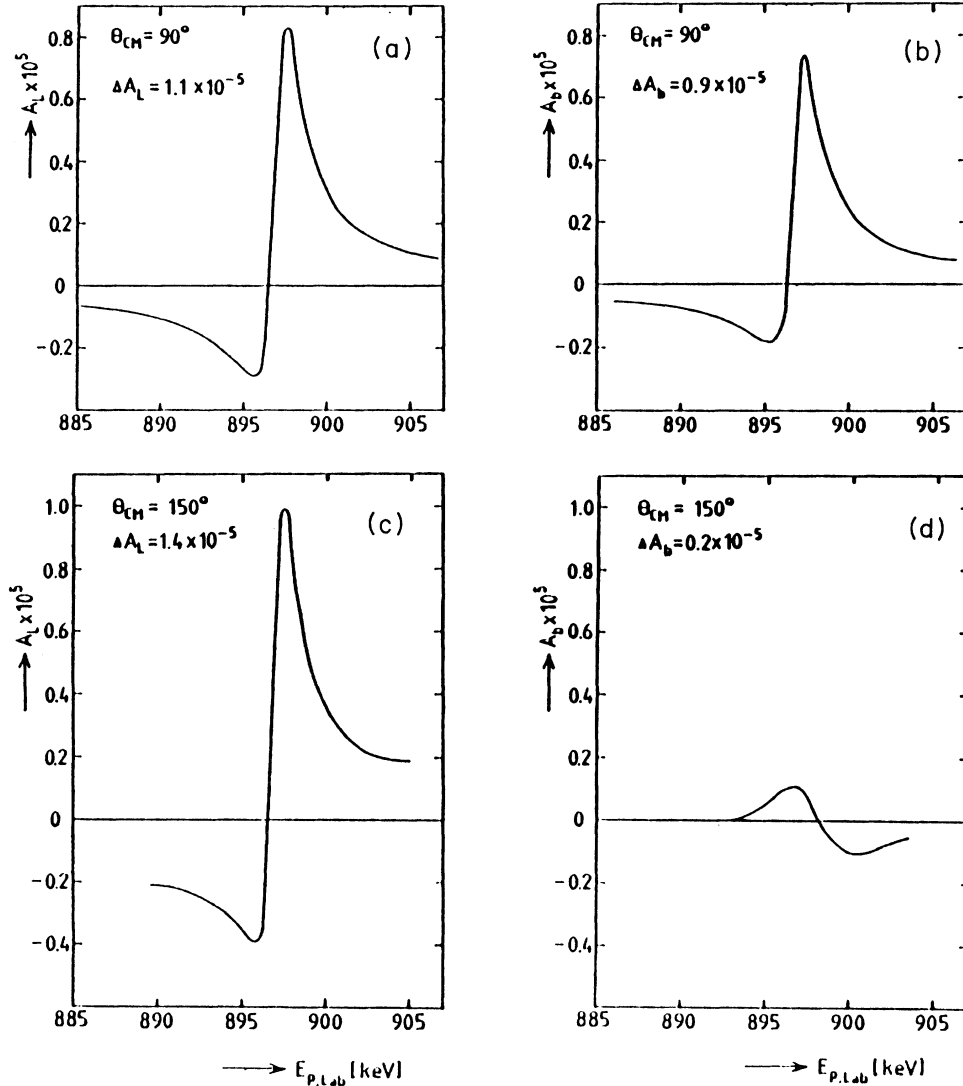
FIG. 5. PNC analyzing powers versus proton energy around the 2^-1 resonance under investigation: (a) A_L at $\theta=90°$, (b) A_b at $\theta=90°$, (c) A_L at $\theta=150°$, and (d) A_b at $\theta=150°$.

TABLE VI. Experimentally [18] and theoretically determined Legendre polynomial coefficients to describe the differential cross section and analyzing power A_n at $E_p = 900$ keV.

	b_1	b_2	a_1
Experiment	-0.813	-0.068	0.087
Theory	-0.801	-0.067	0.038

neither on the phase $\phi_{\rm PNC}$ nor on the PC phase $\phi_{L(b)}$ of $C_{L(b)}$ [see Eq. (19)]. The information on the modulus of the PNC matrix element can therefore be extracted from $A_{L(b)}$ measurements.

One main result of the present contribution can be condensed in the formula

$$\Delta A_{L(b)} = D_{L(b)}^0 \sum_{s=\pi,\rho,\omega} V_s^{\rm PNC} , \qquad (25)$$

where

$$D_{L(b)}^0 = 2(\Gamma^{2^-})^{-1}(\Gamma_p^{2^-}/2\Gamma_p^{2^+})^{1/2}|C_{L(b)}| . \qquad (26)$$

$V_s^{\rm PNC}$ are different meson contributions to the total PNC shell-model matrix element $\langle 2^-1|H_{\rm PNC}|2^+0\rangle$:

$$V_\pi^{\rm PNC} = \frac{1}{4\sqrt{2}} g_\pi h_\pi M_{0,\pi} , \qquad (27)$$

$$V_\rho^{\rm PNC} = -\tfrac{1}{4} g_\rho h_\rho^1 [M_{1,\rho} - M_{3,\rho} + (1+\mu_v) M_{2,\rho}] , \qquad (28)$$

$$V_\omega^{\rm PNC} = -\tfrac{1}{4} g_\omega h_\omega^1 [M_{1,\omega} + M_{3,\omega} + (1+\mu_s) M_{2,\omega}] , \qquad (29)$$

$$V_{\rho'}^{\rm PNC} = -\tfrac{1}{4} g_\rho h_\rho'^1 M_{0,\rho} , \qquad (30)$$

where

$$M_{k,s} = \langle 2^-1|f_{k,s}|2^+0\rangle , \qquad (31)$$

in which

$$f_{0,s} = \frac{1}{M_N} i[\tau_1 \times \tau_2]_z (\sigma_1 + \sigma_2)\mathbf{u}(\mathbf{r},m_s) , \qquad (32)$$

$$f_{1,s} = \frac{1}{M_N}(\tau_{1_z} + \tau_{2_z})(\sigma_1 - \sigma_2)\mathbf{v}(\mathbf{r},m_s) , \qquad (33)$$

$$f_{2,s} = \frac{1}{M_N}(\tau_{1_z} + \tau_{2_z}) i(\sigma_1 \times \sigma_2)\mathbf{u}(\mathbf{r},m_s) , \qquad (34)$$

$$f_{3,s} = \frac{1}{M_N}(\tau_{1_z} - \tau_{2_z})(\sigma_1 + \sigma_2)\mathbf{v}(\mathbf{r},m_s) , \qquad (35)$$

with

$$\mathbf{u}(\mathbf{r},m_s) = \left[(\mathbf{p}_1 - \mathbf{p}_2), \frac{1}{4\pi r}\exp(-m_s r) \right]_- ,$$

$$\mathbf{v}(\mathbf{r},m_s) = \left[(\mathbf{p}_1 - \mathbf{p}_2), \frac{1}{4\pi r}\exp(-m_s r) \right]_+ . \qquad (36)$$

The above formulas gather different ingredients from nuclear reaction theory $(D_{L(b)}^{(0)})$, shell-model matrix elements $(M_{k,s}$; see Table VII), and MNN weak and strong couplings, which contain informations from models describing the interaction between hadrons (see, e.g., Table 2 from Ref. [13]). Therefore, these formulas may be useful for further investigations.

For the longitudinal analyzing power at $\theta_{\rm c.m.} = 90°$, the result $D_L^0 = 1.121 \times 10^{-4}$ eV^{-1} is found. The corresponding value for the irregular transverse analyzing power turns out to be $D_b^0 = 0.92 \times 10^{-4}$ eV^{-1}, while for $\theta_{\rm c.m.} = 150°$, $D_L^0 = 1.4 \times 10^{-4}$ eV^{-1} and $D_b^0 = 0.25 \times 10^{-4}$ eV^{-1} have been obtained. It is interesting to take as examples two limiting cases of strong-interaction constants. One is the case of usual strong couplings of DDH and AH for which the following dependence of ΔA_L on the weak-coupling constants is obtained:

$$\Delta A_L(150°) = 102.39 h_\pi - 5.75 h_\rho^1 - 14.3 h_\omega^1 - 2.15 h_\rho'^1 . \qquad (37)$$

Using the weak coupling of AH (see Table III), the following value for the quoted observable has been obtained:

$$\Delta A_L(150°) = 2.5 \times 10^{-5} . \qquad (38)$$

The other case is the KM strong-coupling one, for which

$$\Delta A_L(150°) = 126.37 h_\pi - 9.46 h_\rho^1 - 12.83 h_\omega^1 - 2.45 h_\rho'^1 , \qquad (39)$$

the final result being

$$\Delta A_L(150°) = 0.43 \times 10^{-5} . \qquad (40)$$

In both examples the small values of the REWIL structure calculation (see Table VII) have been used.

On the basis of these predictions, an experimental proposal to measure the PNC analyzing powers A_L (and A_b) in the ^{15}N$(\vec{p},\alpha_0)^{12}$C reaction is sketched in the following. At backward-scattering angles the (PC) analyzing power A_n is very small or even zero [18], whereas the cross section is maximal in the relevant energy region around $E_{\rm res}(2^-1) \approx E_p = 898$ keV. The situation is favorable for PNC asymmetry measurements because several PC asym-

TABLE VII. Nuclear structure part of the PNC-NN matrix element (in MeV) as defined in Eq. (31) in the text.

	$M_{0,\pi}$	$M_{1,\rho(\omega)}$	$M_{2,\rho(\omega)}$	$M_{3,\rho(\omega)}$	$M_{0,\rho}$
REWIL	0.3076	0.0184	0.0207	0.0192	0.0220
ZWM	0.6569	0.0410	0.0479	0.0383	0.0447

metry effects, superimposed on the PNC observables, are small if A_N is small. Moreover, this advantage coincides with the maximum of the predicted PNC interference effect in A_L [e.g., $\Delta A_L(\theta_{c.m.} = 160°) = 2.6 \times 10^{-5}$]. Although the size of the quantity A_b is smaller than A_L [3,8] in many experimental cases, it has a comparable size near $\theta = 90°$ (see Fig. 5). However, at this angle the differential cross section appears to be smaller (see Fig. 4). Therefore, and because of the solid-angle restriction in the A_b measurement (detectors only in one reaction plane), the observable A_L is the more favorable one for the realization of a PNC experiment.

The small width of the 2^- level at $E_p = 898$ keV requires a thin ^{15}N target ($\Delta E \le 1$ keV) for $E_p = 898$ keV), e.g., realized by implanting ^{15}N ions in the surface of a Ti backing or preparing a thin Ti^{15}N-target layer, as has been used in Ref. [42]. Another possibility is the use of a ^{15}N-gas target. It has the advantage that the energy loss in the target gas can be adjusted in a way that one is able to measure five different energy points around the resonance energy simultaneously. In this case up to 20 Si surface-barrier detectors (or parallel-plate avalanche counters) can be installed in five rings around a long target gas tube, e.g., at $\theta_{lab} = (135 \pm 24)°$ or $\theta_{lab} = (90 \pm 24)°$, as well as at lower energies with large solid angles ($0.4 \le \Omega \le 0.6$sr). The azimuthal angles $\phi = 0°$, $90°$, $180°$, and $270°$ have been chosen to be sensitive for (on-line) monitoring of spurious asymmetries caused by residual transverse polarization components of the beam. The scattered particles leave the gas tube through aluminum foils ($12-15\mu$m), which are used in front of the detectors in order to stop elastically scattered protons and low-energy α_1 particles from excited ^{12}C states, providing background-free α_0 spectra. The reaction energy can be adjusted precisely by detecting the γ rays from the ^{15}N($\vec{p}, \gamma$)^{16}O* reaction. These spectra serve at the same time as a monitor for detecting carbon built-up products on the entrance foil of the gas tube, to correct for this time-dependent additional energy loss of the proton beam. The entrance foil is a self-supporting carbon layer of ≤ 60 nm thickness in order to minimize the energy loss and straggling of the proton beam. This is essential because of the small resonance width of the 2^- level. Selecting an energy resolution of the polarized proton beam of $\approx \pm 0.6$ keV provided by two narrow feedback slit systems and adjusting the target gas pressure to ≈ 1.3 mbar, the measurement can be performed at five energies simultaneously within the interval $E_{res} - \Gamma < E_p < E_{res} + \Gamma$. With an experimental setup of this type, a statistical accuracy of $\approx 0.7 \times 10^{-5}$ will be reached for A_L (135 ± 24)° and A_L (90 ± 24)° after 48μA d of integrated beam charge, if the helicity of the proton beam is switched between $\pm P_z$ with $P_z \ge 0.70$. In order to achieve a sufficient experimental accuracy, the experiment requires a proton beam with high intensity, polarization, and energy resolution. Experiments along these lines are being prepared to the Giessen Tandem Laboratory to investigate the feasibility to measure the PNC anomaly in the longitudinal (and PNC transverse) analyzing powers.

VI. CONCLUSION AND OUTLOOK

It has been shown that measurements of the longitudinal and irregular transverse analyzing powers of the ^{15}N($\vec{p}, \alpha_0$)^{12}C resonance reaction in the excitation energy range near 13 MeV can provide very sensitive and interpretable experiments to determine the PNC matrix element connecting an even-J–odd-parity two-level ($2^-1, 2^+0$) system. The $\langle 2^-1 | H_{PNC} | 2^+0 \rangle$ matrix element has been calculated within the OXBASH code using eight strong- and four weak-interaction models. A conservative value of 0.1 eV has been selected to predict the experimentally relevant observables A_L and A_b, showing a dispersionlike interference pattern in the excitation energy around the 2^-1 resonance. This new ^{16}O case enlarges the number of two-level systems solely sensitive to isovector parity mixing and accessible experimentally with two independent polarization observables.

Measurements of the longitudinal and irregular transverse analyzing powers have been reported in ($\vec{p}, \alpha$) reactions involving the ^{20}Ne compound nucleus [4,5,17]. From the theoretical point of view, the above-proposed PNC α_0 transition from ^{16}O* to ^{12}C(g.s.) may be a better candidate to study isovector parity mixing than the recently investigated similar case from ^{20}Ne to ^{16}O(g.s.). In the latter one the parity- and isospin-forbidden α_0 decay from ^{20}Ne (1^+1, 13.482 MeV) to ^{16}O(g.s.) has been investigated by measurement of the longitudinal and transverse analyzing power via the ^{19}F($\vec{p}, \alpha_0$)^{16}O resonance reaction wherein a close-lying ($\Delta E = 20$ keV) 1^-0 state is involved in the PNC transition. One explanation sustaining the proposed $2^-, 2^+$ doublet in ^{16}O* as a more suitable candidate is the small degree of center-of-mass spuriosity in the calculated structure of the involved ^{16}O levels participating in the ^{15}N($\vec{p}, \alpha_0$)^{12}C resonance reaction. The spuriosity turns out to be very small for the ^{16}O nucleus in comparison with the weight of the spurious-state contribution in the structure of the ^{20}Ne levels, participating in the ^{19}F($\vec{p}, \alpha_0$)^{16}O resonance reaction. Furthermore, the 1^+ state involved in this process is the fifth excited 1^+ level, and shell-model predictions for such highly excited states are clouded by incertitudes. Moreover, this case does not seem to be a simple $1^+, 1^-$ doublet because at least one second 1^- excited state ($\Delta E = 37$ keV) is expected to be involved [4,5]. Since this group of 1^- levels contains the eighth and ninth 1^- excited level of the ^{20}Ne nucleus, an enlarged calculation is necessary for the ^{20}Ne case.

Another two-level system in the ^{14}N compound nucleus [3] has recently been proposed, which is experimentally investigated via elastic scattering of polarized protons in the ^{13}C+p channel (A_L). Although the calculations gave a PNC matrix element being larger by one order of magnitude (using the DDH best values), the predicted interference effect is comparable in size with the predictions for the ^{15}N($\vec{p}, \alpha_0$)^{12}C reaction. However, no isovector terms contribute in the ^{14}N case.

Because of the small level spacing ($\Delta E = 51$ keV), the above-discussed $2^-1, 2^+0$ doublet in ^{16}O* will also be investigated theoretically and experimentally in elastic ^{15}N($\vec{p}, p$)^{15}N scattering via the observables A_L and A_b.

Note added in proof. The matrix elements in Fig. 3, Tables IV and VII, and the right sides of formulas (37)–(40) must be multiplied by a factor 2 which originates from the different parametrization of the PNC potential, for instance Refs. [12] and [1]; the conclusions of Fig. 5 are not changed.

ACKNOWLEDGMENTS

*Permanent address: Department of Fundamental Physics, Institute of Physics and Nuclear Engineering, Institute for Atomic Physics, POB MG-6, Magurele, Bucharest, R-76900, Romania.

[1] E. G. Adelberger and W. C. Haxton, Annu. Rev. Nucl. Part. Sci. **35**, 501 (1985).

[2] S. Kistryn et al., Phys. Rev. Lett. **58**, 1616 (1987).

[3] E. G. Adelberger, P. Hoodbhoy, and B. A. Brown, Phys. Rev. C **30**, 456 (1984); **33**, 1840 (1986).

[4] N. Kniest, E. Huttel, E. Pfaff, G. Reiter, and G. Clausnitzer, Phys. Rev. C **41**, 1337 (1990), and references therein.

[5] N. Kniest, E. Huttel, E. Pfaff, G. Reiter, and G. Clausnitzer, Phys. Rev. C **27**, 906 (1983).

[6] O. Dumitrescu, M. Horoi, F. Carstoiu, and Gh. Stratan, Phys. Rev. C **41**, 1462 (1990); Report No. ICTP Trieste IC/89/8, 1989.

[7] P. G. Bizzeti and P. R. Maurenzig, Nuovo Cimento A **56**, 492 (1980).

[8] P. G. Bizzeti, Phys. Rev. C **33**, 1837 (1986).

[9] F. Ajzenberg-Selove, Nucl. Phys. **A460**, 1 (1986).

[10] D. A. Varshalovitsh, A. N. Moskalev, and V. K. Hersonskii, *Quantum Theory of Angular Momentum* (World Scientific, Singapore, 1989).

[11] H. H. Barshall and H. Haeberli, *Polarization Phenomena in Nuclear Reactions* (University of Wisconsin Press, Madison, 1971).

[12] B. A. Brown, A. Etchegoyen, and W. D. M. Rae, MSU-NSLL Report No. 524, 1985; B. A. Brown, W. E. Ormand, J. S. Winfield, L. Zhao, A. Etchegoyen, W. M. Rae, N. S. Godwin, W. A. Richter, and C. D. Zimmerman, MSU-NSLL Report No. 524, 1988 (Michigan State University version of the OXBASH code).

[13] F. Carstoiu, O. Dumitrescu, G. Stratan, and M. Braic, Nucl. Phys. **A441**, 221 (1985).

[14] O. Dumitrescu, Fiz. Elem. Chastits At. Yadra **10**, 377 (1979) [Sov. J. Part. Nucl. **10**, 147 (1979)].

[15] B. Desplanques, J. F. Donoghue, and B. R. Holstein, Ann. Phys. (N.Y.) **124**, 449 (1980).

[16] N. Kaiser and U. G. Meissner, Nucl. Phys. **A499**, 699 (1989).

[17] J. Ohlert, O. Traudt, and H. Wäffler, Phys. Rev. Lett. **47**, 475 (1981).

[18] G. H. Pepper and L. Brown, Nucl. Phys. **A260**, 163 (1976);

K. H. Bray, A. D. Frawley, T. R. Ophel, and F. C. Barker, ibid. **A288**, 334 (1977).

[19] W. C. Haxton (private communication).

[20] A. P. Zuker, B. Buck, and J. B. McGrory, Phys. Rev. Lett. **21**, 39 (1968); BNL Report No. 14085, 1969.

[21] T. T. S. Kuo and G. E. Brown, Nucl. Phys. **85**, 40 (1966).

[22] J. B. McGrory and B. H. Wildenthal, Phys. Rev. C 7, 954 (1973); Annu. Rev. Nucl. Sci. **30**, 383 (1980).

[23] S. Cohen and D. Kurath, Nucl. Phys. **A73**, 1 (1965).

[24] O. Preedom and B. H. Wildenthal, Phys. Rev. C 6, 1633 (1972).

[25] D. J. Millener and D. Kurath, Nucl. Phys. **A255**, 315 (1975).

[26] B. H. Wildenthal, Prog. Part. Nucl. Phys. **11**, 5 (1984).

[27] B. A. Brown et al., Ann. Phys. (N.Y.) **182**, 191 (1988).

[28] J. B. McGrory and B. H. Wildenthal, Phys. Lett. **60B**, 5 (1975).

[29] D. H. Gloekner and D. R. Lawson, Phys. Lett. **53B**, 313 (1974).

[30] B. A. Brown, W. A. Richter, and N. S. Godwin, Phys. Rev. Lett. **45**, 1681 (1980).

[31] G. A. Miller and J. E. Spencer, Ann. Phys. (N.Y.) **100**, 562 (1976).

[32] O. Dumitrescu, M. Gari, H. Kuemmel, and J. G. Zabolitzky, Z. Naturforsch. A **27**, 733 (1972); Phys. Lett. **35B**, 19 (1971).

[33] M. Gari, Phys. Rep. C 6, 317 (1973).

[34] M. A. Box and B. H. J. Keller, J. Phys. G **11**, 803 (1976).

[35] D. Tadic, Rep. Prog. Phys. **43**, 67 (1980).

[36] V. M. Dubovik and S. V. Zenkin, Ann. Phys. (N.Y.) **172**, 100 (1986); V. M. Dubovik, S. V. Zenkin, I. T. Obukhovskii, and L. A. Tosunyan, Fiz. Elem. Chastits At. Yadra **18**, 575 (1987) [Sov. J. Part. Nucl. **18**, 244 (1987)].

[37] J. Lang, Th. Maier, R. Müller, F. Nessi-Tedaldi, Th. Roser, M. Simonius, J. Sromicki, and W. Haeberli, Phys. Rev. C **34**, 1545 (1986).

[38] R. R. Silbar, W. M. Kloet, L. S. Kisslinger, and J. Dubach, Phys. Rev. C **40**, 2218 (1989).

[39] I. Caprini and L. Micu, Phys. Rev. C **37**, 2209 (1988).

[40] G. Bertsch, J. Borisowicz, H. McManus, and W. G. Love, Nucl. Phys. **A284**, 399 (1977).

[41] J. P. Elliott, A. D. Jackson, H. A. Mavromatis, E. A. Sanderson, and B. Singh, Nucl. Phys. **A121**, 241 (1976).

[42] A. Redder et al., Z. Phys. A **305**, 325 (1982).